ISIJ International, Vol. 57 (2017), No. 10, pp. 1718–1724

Activities of FeO and P_2O_5 in Dephosphorization Slags Coexisting with Solid Solutions between Di-calcium Silicate and Tri-calcium Phosphate

Ryota MATSUGI,[1] Kohei MIWA[2] and Masakatsu HASEGAWA[1]*

1) Department of Energy Science and Technology, Kyoto University, Yoshida-honmachi, Sakyo-ku, Kyoto, 606-8501 Japan.
2) Graduate Student, Kyoto University, Now at Dowa Holdings Co., Ltd., 4-14-1 Sotokanda, Chiyoda-ku, Tokyo, 101-0021 Japan.

(*Received on February 12, 2017; accepted on June 19, 2017*)

Towards better understanding of the phosphorus removal from hot metal with low-basicity slags, electrochemical technique incorporating MgO-stabilized zirconia was conducted to measure simultaneously the activities of FeO and P_2O_5 within heterogeneous CaO–SiO_2–P_2O_5–FeO slags. The FeO activity was fairly insensitive to the variation of $Ca_3P_2O_8$ content in solid solutions between Ca_2SiO_4–$Ca_3P_2O_8$, while the P_2O_5 activity increased with an increase in $Ca_3P_2O_8$ content. By using the present values for activities, phosphorus distribution ratios were estimated between molten slag and carbon-saturated iron. The relationship between phosphorus distribution ratio and FeO content in molten slag was consistent with the phase diagram of the pseudo-ternary CaO–(SiO_2+P_2O_5)–FeO system.

KEY WORDS: dephosphorization; activity; di-calcium silicate; tri-calcium phosphate; solid solution.

1. Introduction

Phosphorus removal from molten iron is an oxidation reaction and formulated as follows.

$$2\left[\mathrm{P}\right]_{\mathrm{Fe}} + 5\left(\mathrm{FeO}\right)_{\mathrm{slag}} = \left(\mathrm{P_2O_5}\right)_{\mathrm{slag}} + 5\left\{\mathrm{Fe}\right\} \quad \text{..... (1)}$$

$$\log K\left(1\right) = \log\left(a_{P_2O_5} / h_P^2\ a_{FeO}^5\right) = -15.48 + 5\,026 / \left(T / \mathrm{K}\right) \quad \text{[1–4)}$$

$$\text{..... (2)}$$

, where $[P]_{Fe}$ is phosphorus in liquid iron, $(FeO)_{slag}$ and $(P_2O_5)_{slag}$ represent FeO and P_2O_5 in slag, respectively, and {Fe} is molten iron. According to Le Chatelier's principle, the general thermochemical conditions for effective dephosphorization are high slag basicity (low P_2O_5 activity), high oxygen potential (high FeO activity), and low temperature. It has been also reported that $(P_2O_5)_{slag}$ often is observed in solid solutions between Ca_2SiO_4 and $Ca_3P_2O_8$.[5)]

Based on the considerations mentioned above, a number of the investigations have been conducted to clarify phosphorus distribution ratios between slags and molten iron, and activities of P_2O_5 and FeO in dephosphorization slags. For example, phosphorus distribution ratios between CaO-containing slags and molten iron were measured by Ito and Sano,[6)] Wrampelmeyer *et al*.,[7)] and Im *et al*.[8)] Distributions of oxygen and phosphorus between slags and liquid iron were investigated by Nagabayashi *et al*., and based on their experimental results, they suggested the regular solution model to calculate the activity coefficients of P_2O_5 in FeO–Fe_2O_3–P_2O_5–SiO_2–CaO–MgO slags.[9)] By applying this regular solution model to molten slags coexisted with Ca_2SiO_4–$Ca_3P_2O_8$ solid solutions, Shimauchi *et al*. derived the activity coefficients of P_2O_5 in these solid solutions.[10)] Zhong *et al*. measured the P_2O_5 activities in Ca_2SiO_4–$Ca_3P_2O_8$ solid solutions at 1 823 K and 1 873 K by a chemical equilibrium method in which molten iron was brought into equilibria with oxides under oxygen partial pressures controlled by CO + CO_2 gas mixtures.[11–13)] The present authors determined the P_2O_5 activities by equilibrating molten copper with Ca_2SiO_4–$Ca_3P_2O_8$ solid solution-containing slags under a stream of Ar + H_2 + H_2O gas mixture,[14)] and derived the formulae of the activities of Ca_2SiO_4 and $Ca_3P_2O_8$ in these solid solutions at 1 573 K.[15)] The activities of FeO in CaO-based slags were measured by employing an electrochemical technique involving stabilized zirconia.[16,17)] To the best of authors' knowledge, however, there would be still lack of thermochemical data on the activities of P_2O_5 and FeO in low-basicity slags, which contain Ca_2SiO_4–$Ca_3P_2O_8$ solid solutions, at temperature of hot metal processing.

Figure 1 illustrates the phase relations within the quaternary system of CaO–SiO_2–P_2O_5–FeO at 1 573 K.[18)] In this figure and hereafter, the following abbreviations are used.

$$\mathrm{C_2S} = \mathrm{Ca_2SiO_4} = 2\mathrm{CaO}\cdot\mathrm{SiO_2}$$

$$\mathrm{C_3S_2} = \mathrm{Ca_3Si_2O_7} = 3\mathrm{CaO}\cdot 2\mathrm{SiO_2}$$

$$\mathrm{CS} = \mathrm{CaSiO_3} = \mathrm{CaO}\cdot\mathrm{SiO_2}$$

* Corresponding author: E-mail: hasegawa.masakatsu.7r@kyoto-u.ac.jp
DOI: http://dx.doi.org/10.2355/isijinternational.ISIJINT-2017-082

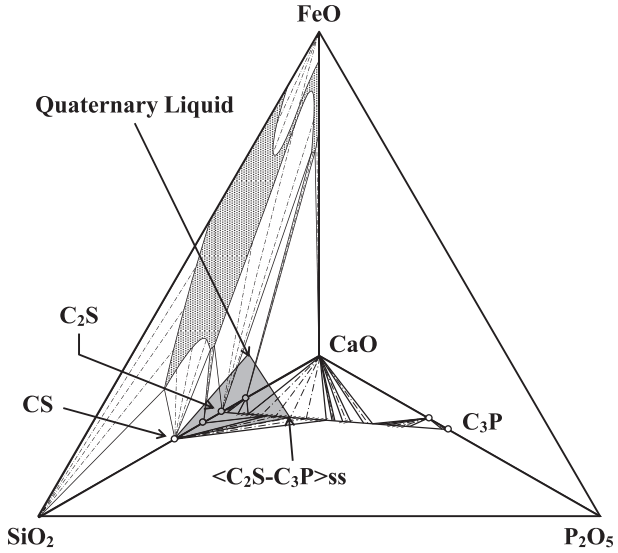

Fig. 1. Schematic diagram of phase relationship in the CaO–SiO_2–P_2O_5–FeO quaternary system at 1 573 K.

$$C_3P = Ca_3P_2O_8 = 3CaO \cdot P_2O_5$$

$$<C_2S - C_3P>ss =$$

solid solution between Ca_2SiO_4 and $Ca_3P_2O_8$

In Fig. 1, the solid solutions near CaO, C_2S and C_3P are not illustrated in order to avoid complexity of the diagram. The base CaO–SiO_2–P_2O_5 and the side CaO–SiO_2–FeO of this tetrahedron represent the phase diagrams of the corresponding ternary systems at 1 573 K,[19,20] respectively. As seen in this figure, <C_2S–C_3P>ss could coexist with solid CaO in basic slags, while it could coexist with CS in low-basicity slags. Therefore, attention is now focused on the 3-phase assemblage of <C_2S–C_3P>ss + CS + {CaO–SiO_2–P_2O_5–FeO} quaternary liquid. In the present study, firstly, by employing electron probe microanalysis (EPMA), the compositions of liquid phase coexisted with <C_2S–C_3P>ss and CS were determined at 1 573 K. The simultaneous determinations for the activities of P_2O_5 and FeO were subsequently conducted by using electrochemical technique.

2. Experimental Aspects

2.1. EPMA Studies

Di-calcium silicate, C_2S, and mono-calcium silicate, CS, were obtained by mixing requisite portions of $CaCO_3$ and SiO_2 and heating at 1 573 K for 24 hours and 98 hours, respectively. Tri-calcium phosphate, C_3P, was obtained from Nacalai Tesque, Inc., Kyoto, Japan, and dried at 413 K. The preparations of <C_2S–C_3P>ss were based on mixing requisite portions of C_2S and C_3P to yield the initial C_3P concentrations of 18, 24, and 31 mass%, respectively, and heating at 1 573 K for 24 hours. The starting materials thus obtained were mixed with iron oxide, and pressed into a steel die. The bulk compositions of the oxide mixtures are given in **Table 1**. Oxide pellets were charged in an iron crucible, and heated to 1 573 K in a stream of purified argon in order to yield the appropriate 3-phase region. The gas purification train for argon consisted of silica-gel, phosphorus pentoxide and magnesium chips held at 823 K. After heating over 48 hours, samples were quenched into liquid nitrogen, submitted, firstly, to X-ray diffraction analysis to confirm expected solid phases, and, subsequently, to EPMA to determine the compositions of solid phases and quaternary liquid phase.

Table 1. Bulk compositions of slag samples.

Initial (*mass%*C_3P) in <C_2S–C_3P>ss	(*mass%CaO*)	(*mass%*SiO_2)	(*mass%*P_2O_5)	(*mass%FeO*)
18	53.5	39.7	3.8	3.0
24	53.2	38.5	5.1	3.1
31	52.8	37.9	6.7	2.5

2.2. Activity Measurements

Figure 2 schematically shows the experimental apparatus. The slag samples used for activity measurements were the same as described in EPMA studies. An iron crucible, 25-mm i.d., 35-mm o.d., and 100-mm height, was charged with 10 g of powdery slag and 40 g of high-purity copper, and heated under a stream of purified argon in a SiC resistance furnace. When the copper was molten, the iron crucible would dissolve into liquid copper to a small extent, to form {Cu–Fe–P} ternary liquid alloy, while <Fe–Cu–P> solid solutions would formed on the inner wall of the iron crucible.

After the temperature reached the desired value, the zirconia electrolyte cell was immersed into {Cu–Fe–P} liquid alloys, and electromotive force (*emf*) measurements were initiated. After the *emf* values remained stable (±0.1 mV) for a period of over 1 hour at a constant temperature, samples were withdrawn from the {Cu–Fe–P} liquid alloy by means of a silica sampling tube of 3-mm i.d. The concentrations of phosphorus in the samples, $[mass\%P]_{Cu-Fe-P}$, were determined by using an inductively-coupled plasma spectrometer. **Figure 3** shows typical records of cell potentials and the compositions of {Cu–Fe–P} liquid alloy. As shown in this figure, durations of about 100 hours were required to attain one equilibrium state. These procedures were repeated at three different initial concentrations of C_3P in <C_2S–C_3P>ss, *i.e.* 18, 24 and 31 mass%. In order to confirm the reproducibility, the experiments were also conducted at three different temperatures, *i.e.* 1 548, 1 573, and 1 598 K. After each experimental run, the iron crucible was submitted to EPMA in order to ensure the presence of <Fe–Cu–P> solid solutions on the inner wall of the crucible.

The open circuit *emf*, *E*, of the cell used in this study is given by[21]

$$E = \frac{RT}{F} \ln \frac{P_{O_2}\left(ref.\right)^{1/4} + P_e^{1/4}}{P_{O_2}^{1/4} + P_e^{1/4}} + E_t \quad \text{..... (3)}$$

, where *E* is cell voltage, E_t is thermo-*emf* between Mo(+) and Fe(−),[22] *R* is the gas constant, *T* is temperature, *F* is the Faraday constant, and P_e is the oxygen partial pressure at which the ionic and the n-type electronic conductivities are equal. Values for this parameter for the magnesia-stabilized zirconia tubes used in this study have been reported elsewhere.[23]

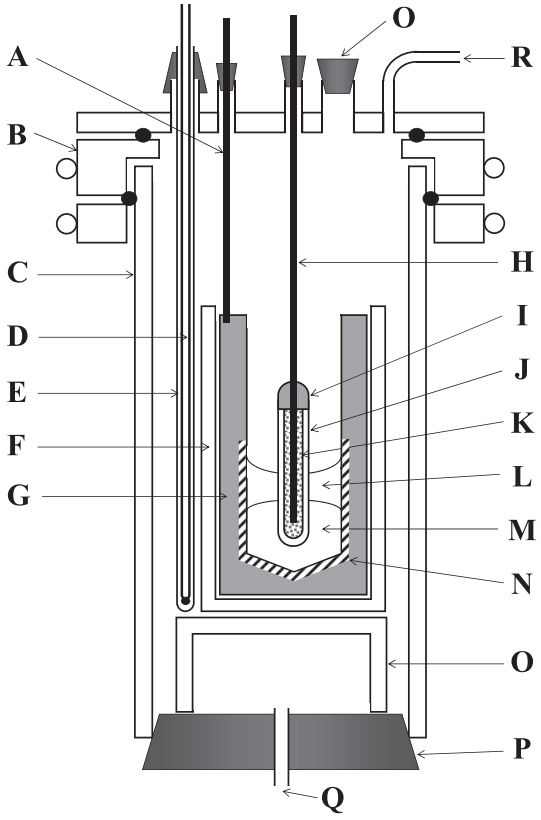

Fig. 2. Experimental apparatus used in this study for the simultaneous measurements of the FeO and P_2O_5 activities. (A) Iron rod, (B) Water-cooled brass flange, (C) Mullite reaction tube, (D) Pt-PtRh13 thermocouple, (E) Alumina sheath, (F) Alumina crucible, (G) Iron crucible, (H) Molybdenum rod, (I) Zirconia cement, (J) ZrO_2(MgO) solid electrolyte tube, (K) Mo + MoO_2 reference electrode, (L) Slag, (M) {Cu–Fe–P} liquid alloy, (N) <Fe–Cu–P> solid alloy, (O) Alumina pedestal, (P) Rubber stopper, (Q) Gas inlet, (R) Gas outlet.

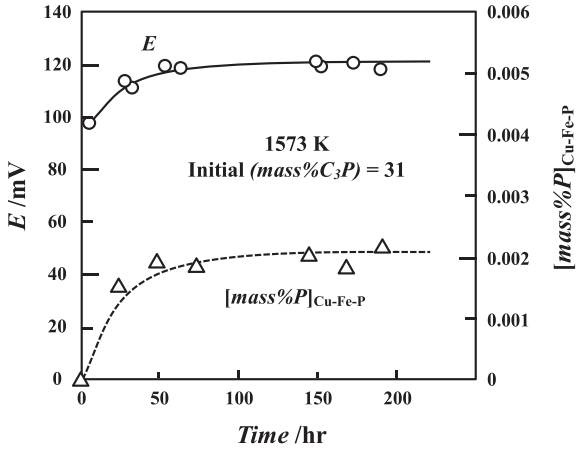

Fig. 3. Typical records of cell potentials and phosphorus contents in {Cu–Fe–P} liquid alloy during an experimental run.

$$\log\left(P_e / \mathrm{atm}\right) = +20.40 - 6.45\times10^4 / \left(T / \mathrm{K}\right) \ldots\ldots (4)$$

The oxygen partial pressures at the reference electrode, Mo + MoO_2, $P_{O_2}(ref.)$, have been measured as[24)]

$$\log\left\{P_{O_2}\left(ref.\right) / \mathrm{atm}\right\} = +8.84 - 30\,100 / \left(T / \mathrm{K}\right) \ldots\ldots (5)$$

By using Eqs. (3) through (5), the equilibrium oxygen partial pressures, P_{O_2}, could be determined between heterogeneous slags and Cu–Fe–P alloys.

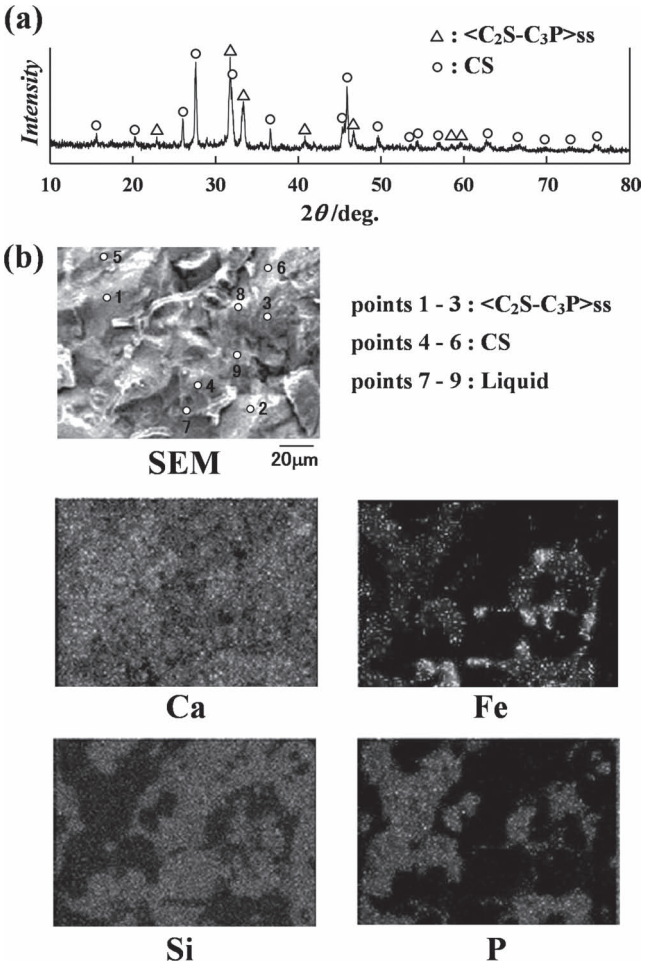

Fig. 4. (a) XRD pattern, and (b) SEM image and mappings of the sample at initial (*mass%C_3P*) = 31.

3. Experimental Results and Discussion

3.1. EPMA Studies

Figure 4 shows the XRD pattern, SEM image and mappings of the sample at initial (*mass%C_3P*) = 31. The XRD pattern indicated that the sample contained <C_2S–C_3P>ss and CS as solid phases, and based on the mappings of Ca, Fe, Si and P, the phases at points 1 to 3, 4 to 6 and 7 to 9 on the SEM image were recognized to be <C_2S–C_3P>ss, CS and quaternary liquid, respectively. XRD and EPMA studies confirmed that all the slags investigated in this study occurred at the expected 3-phase region. The compositions of the three phases, *i.e.* <C_2S–C_3P>ss, CS and {CaO–SiO_2–P_2O_5–FeO} quaternary liquid phase, are numerically given in **Table 2**.

The compositions of {CaO–SiO_2–P_2O_5–FeO} quaternary liquid phase coexisted with <C_2S–C_3P>ss and CS were projected onto the pseudo-ternary system CaO–(SiO_2+P_2O_5)–FeO in **Fig. 5**(a), together with those in the 2-phase assemblages of <C_2S–C_3P>$_{ss}$ + liquid[6)] and CS + liquid.[8)] As shown in this figure, the liquidus compositions determined in this study were consistent with the liquidus lines reported in the literature.

Table 2. Compositions of phases within the 3-phase assemblage at 1 573 K.

Initial (*mass%C_3P*) in <C_2S–C_3P>ss	Phase	(*mass%CaO*)	(*mass%SiO_2*)	(*mass%P_2O_5*)	(*mass%FeO*)	Remark
	<C_2S–C_3P>ss	55.50	29.22	6.56	8.72	(*mass%C_3P*) = 14.33
18	CS	47.44	52.04	0.04	0.49	–
	Liquid	42.68	37.35	2.16	17.82	–
	<C_2S–C_3P>ss	52.48	26.44	9.96	11.12	(*mass%C_3P*) = 21.76
24	CS	46.97	52.59	0.02	0.40	–
	Liquid	42.26	35.70	3.29	18.76	–
	<C_2S–C_3P>ss	53.31	26.16	10.44	10.09	(*mass%C_3P*) = 22.80
31	CS	52.46	45.72	0.86	0.96	–
	Liquid	41.56	38.70	5.11	14.63	–

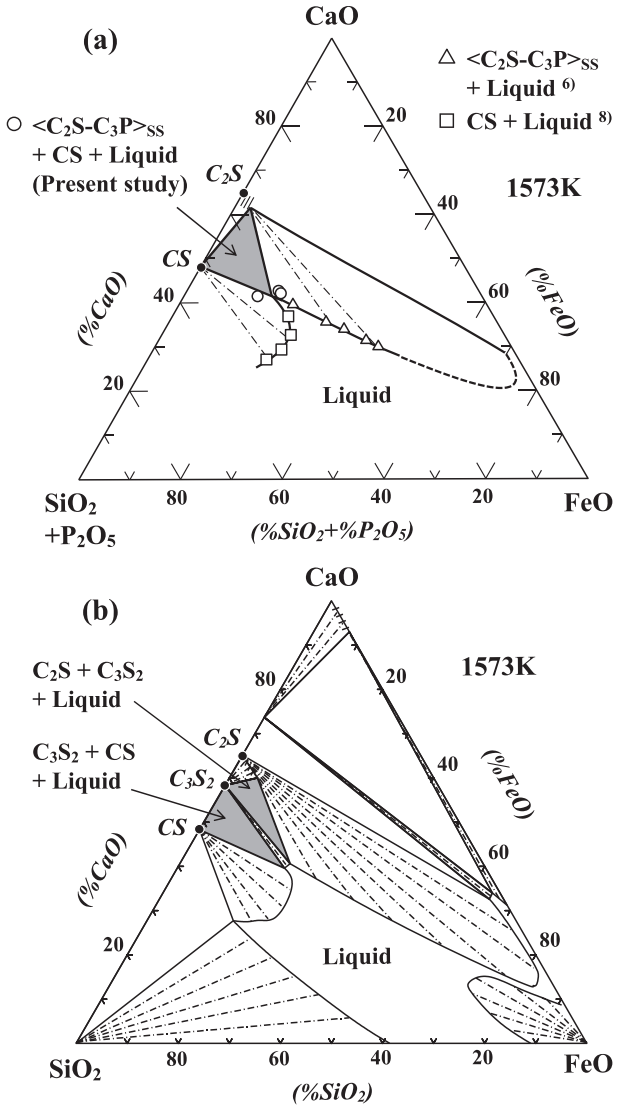

Fig. 5. (a) Phase relationship projected on the CaO–(SiO_2+P_2O_5)–FeO pseudo-ternary field at 1 573 K. (b) Iso-thermal section of the CaO–SiO_2–FeO ternary system at 1 573 K.[20]

3.2. Activity Measurements

As for FeO in the slags, the equilibrium reaction between iron in Cu–Fe–P alloy, $\{Fe\}_{Cu–Fe–P}$, and FeO in slag could be expressed by

$$\{Fe\}_{Cu-Fe-P} + (1/2)O_2\,(gas) = (FeO)_{slag} \quad \text{..... (6)}$$

$$K(6) = a_{FeO} / a_{Fe} P_{O_2}^{1/2} = 1 / P^{\circ}{}_{O_2}{}^{1/2} \quad \text{..... (7)}$$

$$\log a_{FeO} = \log a_{Fe} + (1/2)(\log P_{O_2} - \log P^{\circ}{}_{O_2}) \quad \text{..... (8)}$$

, where a_{Fe} is the activity of iron, and $P^{\circ}{}_{O_2}$ is the equilibrium oxygen partial pressure for the mixture of "pure" non-stoichiometric liquid FeO + pure solid iron.[2]

$$\log(P^{\circ}{}_{O_2} / \text{atm}) = +4.39 - 2.35\times10^4 / (T / \text{K}) \quad \text{..... (9)}$$

Namely, the standard state for FeO was taken as "pure" liquid FeO in equilibrium with pure solid iron. The equilibrium oxygen partial pressure, P_{O_2}, between iron in {Cu–Fe–P} liquid alloy and FeO in slag can be calculated from Eqs. (3) through (5), and values for a_{Fe} in {Cu–Fe–P} liquid alloy at dilute phosphorus concentrations saturated with <Fe–Cu–P> solid alloy have been reported as follows.[25]

$$\log a_{Fe} = -(0.37 \pm 0.12) + (500 \pm 200)/(T / \text{K}) \quad \text{... (10)}$$

Table 3 summarizes the FeO activities in the 3-phase region of <C_2S–C_3P>ss + CS + {CaO–SiO_2–P_2O_5–FeO} quaternary liquid. At a fixed initial (*mass%C_3P*), the FeO activity decreased with an increase in temperature. This would be explained by the expansion of the liquid region to low FeO concentration as temperature increased.

Figure 5(b) shows the iso-thermal section of the CaO–SiO_2–FeO ternary system at 1 573 K.[20] In this figure, there are two 3-phase assemblages of C_2S + C_3S_2 + liquid and C_3S_2 + CS + liquid. When P_2O_5 is added to CaO–SiO_2–FeO ternary slags, these two 3-phase regions would join to form a 3-phase region of <C_2S–C_3P>ss + CS + {CaO–SiO_2–P_2O_5–FeO} quaternary liquid. Hence, it would be of interest to compare the present data for the CaO–SiO_2–P_2O_5–FeO quaternary slags with those for the CaO–SiO_2–FeO ternary slags.[26] In **Fig. 6**, the concentrations and activities of FeO in quaternary and ternary liquid phases at 1 573 K are plotted against the analyzed values for the C_3P concentrations in <C_2S–C_3P>ss. The present values for a_{FeO} in the 3-phase region of <C_2S–C_3P>ss + CS + {CaO–SiO_2–P_2O_5–FeO} quaternary liquid are slightly lower than those in the 3-phase assemblages of C_2S + C_3S_2 + {CaO–SiO_2–FeO} ternary liquid and C_3S_2 + CS + {CaO–SiO_2–FeO} ternary liquid. With respect to this, it is worth noting that the FeO concentrations in quaternary melt coexisted with <C_2S–C_3P>ss +

Table 3. Experimental results for activities of FeO and P_2O_5.

Initial (*mass%C₃P*) in <C_2S–C_3P>ss	*T* /K	*E* /mV	log(P_{O_2}/atm)	a_{FeO}	$[mass\%P]_{Cu-Fe-P}\times10^4$	log $a_{P_2O_5}$
18	1 548	101.61 ± 0.40	−11.66 ± 0.01	0.328 ± 0.002	6.2 ± 0.4	−20.95 ± 0.05
	1 573	118.08 ± 0.45	−11.54 ± 0.01	0.282 ± 0.002	7.8 ± 0.6	−20.96 ± 0.06
	1 598	130.90 ± 0.94	−11.38 ± 0.01	0.257 ± 0.003	21.9 ± 4.0	−20.18 ± 0.20
24	1 548	102.78 ± 0.56	−11.68 ± 0.01	0.323 ± 0.003	6.7 ±0.6	−20.93 ± 0.08
	1 573	115.18 ± 0.28	−11.51 ± 0.00	0.295 ± 0.001	9.6 ± 0.4	−20.71 ± 0.05
	1 598	132.58 ± 0.89	−11.40 ± 0.01	0.251 ± 0.003	34.3 ± 2.6	−19.83 ± 0.04
31	1 548	109.08 ± 1.40	−11.76 ± 0.02	0.294 ± 0.006	16.5 ± 1.9	−20.37 ± 0.08
	1 573	119.51 ± 0.40	−11.56 ± 0.00	0.277 ± 0.001	19.8 ± 0.6	−20.19 ± 0.04
	1 598	135.40 ± 0.86	−11.44 ± 0.01	0.240 ± 0.003	43.6 ± 3.5	−19.71 ± 0.08

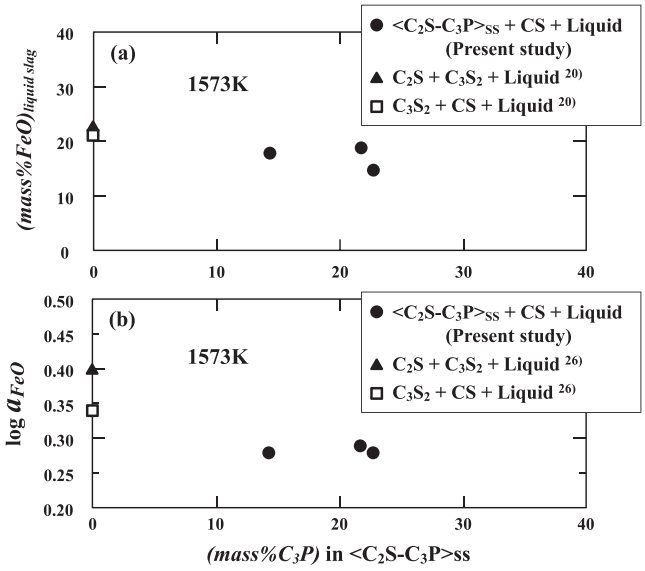

Fig. 6. (a) FeO contents in liquid slags plotted against C_3P contents in <C_2S–C_3P>ss at 1 573 K. (b) FeO activities plotted against C_3P contents in <C_2S–C_3P>ss at 1 573 K.

CS are lower than those in ternary liquid coexisted with C_2S + C_3S_2 or C_3S_2 + CS. As seen in Fig. 6, it could be also concluded that the concentrations and activities of FeO in quaternary liquid phase were fairly insensitive to the variation of the C_3P concentrations in <C_2S–C_3P>ss.

As for P_2O_5 in the slags, the equilibrium reaction between phosphorus in Cu–Fe–P alloy, $\{P\}_{Cu-Fe-P}$, and P_2O_5 in slag could be formulated by

$$2\{P\}_{Cu-Fe-P} + (5/2)O_2(gas) = (P_2O_5)_{slag} \quad \text{..... (11)}$$

$$K(11) = a_{P_2O_5} / h_P^2 P_{O_2}^{5/2} \quad \text{..... (12)}$$

It could be noted here that, in the present experiments, the equilibrium oxygen partial pressures for Eq. (11) were identical to those for Eq. (6). The standard states for the activity of P_2O_5, $a_{P_2O_5}$, and the Henrian activity of phosphorus, h_P, were taken as hypothetical pure liquid P_2O_5 and 1 mass% solution of phosphorus in molten copper, respectively. In {Cu–Fe–P} liquid alloy saturated with <Fe–Cu–P> solid alloy, the activity of phosphorus at dilute phosphorus concentration has been formulated by[27)]

$$\log h_P = \log[mass\%P]_{Cu-Fe-P} + (4.46 \pm 0.40) - (8\,710 \pm 770)/(T/\mathrm{K}) \quad \text{... (13)}$$

Turkdogan and Pearson gave the following.[1)]

$$P_2(gas) + (5/2)O_2(gas) = P_2O_5(liquid) \quad \text{..... (14)}$$

$$\Delta G^\circ(14)/\mathrm{J\cdot mol^{-1}} = -1\,534\,500 + 506.2\times(T/\mathrm{K}) \quad \text{.... (15)}$$

The Gibbs energy changes for the dissolution of diatomic phosphorus into liquid copper at 1 mass% solution are given by[28)]

$$(1/2)P_2(gas) = \{P\}_{Cu} \quad \text{..... (16)}$$

$$\Delta G^\circ(16)/\mathrm{J\cdot mol^{-1}} = -RT\ln(h_P / p_{P_2}^{1/2}) = -125\,000 + 0.54\times(T/\mathrm{K}) \quad \text{..... (17)}$$

By combining Eqs. (15) and (17), the Gibbs energy change for Reaction (11) is given as

$$\Delta G^\circ(11)/\mathrm{J\cdot mol^{-1}} = -RT\ln K(11) = -1\,284\,500 + 505.1\times(T/\mathrm{K}) \quad \text{..... (18)}$$

Hence, $a_{P_2O_5}$ can be obtained by using Eqs. (12), (13) and (18), and are summarized in Table 3. The P_2O_5 activity increased with an increase in temperature. **Figure 7** shows the values for $a_{P_2O_5}$ plotted against the analyzed C_3P concentrations in <C_2S–C_3P>ss at 1 573 K. The P_2O_5 activity in the 3-phase region of <C_2S–C_3P>ss + CS + {CaO–SiO_2–P_2O_5–FeO} quaternary liquid increased with an increase in the C_3P concentration.

In the 3-phase assemblage of <C_2S–C_3P>ss + CS + {CaO–SiO_2–P_2O_5–FeO} quaternary liquid, the equilibrium reactions among the components can be expressed as follows.

$$2CaO + SiO_2 = C_2S \quad \text{..... (19)}$$

$$\log K(19) = \log a_{C_2S} - 2\log a_{CaO} - \log a_{SiO_2} = 4.78 \quad \text{at } 1573\,\mathrm{K}^{3,29)} \quad \text{..... (20)}$$

$$CaO + SiO_2 = CS \quad \text{..... (21)}$$

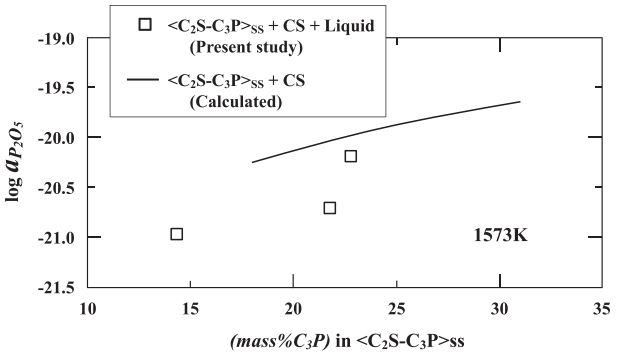

Fig. 7. Logarithmic values for P_2O_5 activities plotted against C_3P contents in $<C_2S–C_3P>$ss at 1 573 K.

$$\log K(21) = -\log a_{CaO} - \log a_{SiO_2} = 2.92 \quad \text{at 1 573 K}^{3,29)} \quad \text{..... (22)}$$

$$3CaO + P_2O_5 = C_3P \quad \text{..... (23)}$$

$$\log K(23) = \log a_{C_3P} - 3\log a_{CaO} - \log a_{P_2O_5} = 24.80 \quad \text{at 1573 K}^{1,30,31)} \quad \text{..... (24)}$$

, where the activity of CS is considered to be unity. Combining Eqs. (20), (22) and (24), we obtain

$$\log a_{P_2O_5} = \log a_{C_3P} - 3\log a_{C_2S} - 19.22 \quad \text{at 1 573 K} \quad \text{..... (25)}$$

Equation (25) implies that the P_2O_5 activity in the 3-phase region would increase as the C_3P content in $<C_2S–C_3P>$ss increases at a constant temperature, due to an increase in the C_3P activity and a decrease in the C_2S activity. Therefore, the relationship between $a_{P_2O_5}$ and C_3P content illustrated in Fig. 7 was thermodynamically consistent with Eq. (25).

By the present authors, the C_2S and C_3P activities in $<C_2S–C_3P>$ss at 1 573 K have been formulated as[15)]

$$\log a_{C_2S} = 3.76\times10^{-2} + \log(1-Y) + 1.91\times10^{-1}\times Y^2 \quad \text{... (26)}$$

$$\log a_{C_3P} = 6.80\times10^{-3} + 2\log Y + 3.81\times10^{-1}\times(1-Y)^2 \quad \text{..... (27)}$$

, where Y represents the substitution ratio and is defined by

$$Y = 2n_{C_3P} / (n_{C_2S} + 2n_{C_3P}) \quad \text{..... (28)}$$

In Eq. (28), n_i denotes the number of moles of component i in solid solutions. Then, the P_2O_5 activity in $<C_2S–C_3P>$ss coexisted with CS can be calculated from Eqs. (25), (26) and (27), and is shown by a solid line in Fig. 7. The P_2O_5 activities in the 3-phase region of $<C_2S–C_3P>$ss + CS + {CaO–SiO_2–P_2O_5–FeO} quaternary liquid are lower than that in the 2-phase region of $<C_2S–C_3P>$ss + CS; this would be affected by the dissolution of FeO into $<C_2S–C_3P>$ss in the CaO–SiO_2–P_2O_5–FeO quaternary system, as seen in Table 2.

3.3. Phosphorus Distribution Ratio

By rewriting Eq. (2), we have

$$\log h_P = -(1/2)\log K(1) + (1/2)\log a_{P_2O_5} - (5/2)\log a_{FeO} \quad \text{..... (29)}$$

For carbon-saturated {Fe–C–P} liquid alloys, the Henrian activity of phosphorus is given by

Table 4. Estimated phosphorus contents in molten iron attainable with the heterogeneous slags.

Initial (*mass%C3P*) in $<C_2S–C_3P>$ss	*T* /K	log[*mass%P*]$_{Fe}$
18	1 573	−2.93 ± 0.09
24	1 573	−2.84 ± 0.07
31	1 573	−2.54 ± 0.05

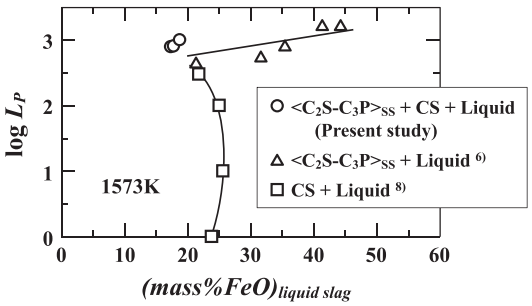

Fig. 8. Relationship between phosphorus distribution ratio and FeO content in liquid slag at 1 573 K.

$$\log h_P = \log[mass\%P]_{Fe} + e_P^C[mass\%C]_{Fe} + e_P^P[mass\%P]_{Fe} \quad \text{..... (30)}$$

, where e_i^j is the first order interaction coefficient in liquid iron[4,32)] and $[mass\%C]_{Fe}$ is the carbon concentration in liquid iron saturated with solid carbon. Combining Eqs. (2), (29) and (30), we have

$$\begin{aligned}\log[mass\%P]_{Fe} + e_P^P[mass\%P]_{Fe} &= -e_P^C[mass\%C]_{Fe} - (1/2)\log K(1) \\ &\quad + (1/2)\log a_{P_2O_5} - (5/2)\log a_{FeO} \\ &= -e_P^C[mass\%C]_{Fe} + (1/2)\log a_{P_2O_5} \\ &\quad - (5/2)\log a_{FeO} + 7.74 - 2\,513/(T/\mathrm{K})\end{aligned} \quad \text{... (31)}$$

The equilibrium phosphorus concentrations, $[mass\%P]_{Fe}$, attainable with the heterogeneous slags of $<C_2S–C_3P>$ss + CS + {CaO–SiO_2–P_2O_5–FeO} quaternary liquid can be estimated by inserting the present values for a_{FeO} and $a_{P_2O_5}$ to Eq. (31). The calculation results given in **Table 4** indicated that it would be possible to lower the equilibrium phosphorus level less than 100 ppm in phosphorus removal conducted with these heterogeneous slags.

Phosphorus distribution ratio, L_P, is defined by the following expression.

$$L_P = (mass\%P)_{\text{liquid slag}} / [mass\%P]_{\text{Fe}} \quad \text{..... (32)}$$

, where $(mass\%P)_{\text{liquid slag}}$ and $[mass\%P]_{\text{Fe}}$ denote the concentrations of phosphorus in liquid slag and in carbon-saturated iron, respectively. For the 3-phase assemblage of $<C_2S–C_3P>$ss + CS + {CaO–SiO_2–P_2O_5–FeO} quaternary liquid, the former can be derived from the P_2O_5 concentration in liquid phase given in Table 2, while the latter is given in Table 4. **Figure 8** shows the present values for logL_P at 1 573 K plotted against the FeO contents in liquid phase. For comparison, this figure also illustrates logL_P along

the liquidus lines coexisted with $<C_2S–C_3P>_{ss}$[6] and CS.[8] Based on the consideration that value for $\log L_P$ increases with an increase in slag basicity or oxygen potential, it could be concluded that the relationships between $\log L_P$ and FeO content along the liquidus lines shown in Fig. 8 are not inconsistent with the phase relations in Fig. 5(a).

4. Conclusion

In the present study, attention was focused on the 3-phase assemblage within the $CaO–SiO_2–P_2O_5–FeO$ quaternary system; $Ca_2SiO_4–Ca_3P_2O_8$ solid solution + $CaSiO_3$ + quaternary liquid. Firstly, the compositions of solid and liquid phases were determined through EPMA, and subsequently, the activities of FeO and P_2O_5 were measured simultaneously by virtue of an electrochemical technique incorporating magnesia-stabilized zirconia. Thermochemical consistency was observed between activities and EPMA studies. Based on the present data, the equilibrium phosphorus content in carbon-saturated iron and phosphorus distribution ratio were estimated. There was a possibility to remove phosphorus less than 100 ppm by using low-basicity slags investigated in this study.

Acknowledgement

This work was supported by ISIJ and JSPS KAKENHI Grant Number 15K06524, and these are gratefully acknowledged.

REFERENCES

1) E. T. Turkdogan and J. Pearson: *J. Iron Steel Inst.*, **175** (1953), 393.
2) M. Iwase, N. Yamada, K. Nishida and E. Ichise: *Trans. Iron Steel Soc. AIME*, **4** (1984), 69.
3) O. Kubaschewski, C. B. Alcock and P. J. Spencer: Materials Thermochemistry, 6th Ed., Pergamon Press, Oxford, (1993), 257.
4) G. K. Sigworth and J. F. Elliott: *Met. Sci.*, **8** (1974), 298.
5) H. Suito, Y. Hayashida and Y. Takahashi: *Tetsu-to-Hagané*, **63** (1977), 1252.
6) K. Ito and N. Sano: *Tetsu-to-Hagané*, **69** (1983), 1746.
7) J.-C. Wrampelmeyer, S. Dimitrov and D. Janke: *Steel Res.*, **60** (1989), 539.
8) J. Im, K. Morita and N. Sano: *ISIJ Int.*, **36** (1996), 517.
9) R. Nagabayashi, M. Hino and S. Ban-ya: *ISIJ Int.*, **29** (1989), 140.
10) K. Shimauchi, S. Kitamura and H. Shibata: *Tetsu-to-Hagané*, **95** (2009), 229.
11) M. Zhong, H. Matsuura and F. Tsukihashi: *Mater. Trans.*, **56** (2015), 1192.
12) M. Zhong, H. Matsuura and F. Tsukihashi: *ISIJ Int.*, **55** (2015), 2283.
13) M. Zhong, H. Matsuura and F. Tsukihashi: *Metall. Mater. Trans. B*, **47B** (2016), 1745.
14) H. Takeshita, M. Hasegawa, Y. Kashiwaya and M. Iwase: *Steel Res. Int.*, **81** (2010), 100.
15) M. Hasegawa, Y. Kashiwaya and M. Iwase: *High Temp. Mater. Process.*, **31** (2012), 421.
16) M. Hasegawa, M. Iwase, K. Wakimoto and A. McLean: *Scand. J. Metall.*, **32** (2003), 47.
17) M. Hasegawa and M. Iwase: *Tetsu-to-Hagané*, **95** (2009), 222.
18) R. Matsugi, K. Miwa and M. Hasegawa: *CAMP-ISIJ*, **28** (2015), 660, CD-ROM.
19) M. Matsu-sue, M. Hasegawa, K. Fushi-tani and M. Iwase: *Steel Res. Int.*, **78** (2007), 465.
20) A. Muan and E. F. Osborn: Phase Equilibria among Oxides in Steelmaking, Addison-Wesley Publishing, Reading, MA, (1965), 113.
21) H. Schmalzried: *Z. Elektrochem.*, **66** (1962), 572.
22) M. Iwase, N. Yamada, E. Ichise and H. Akizuki: *Trans. Iron Steel Soc. AIME*, **5** (1984), 53.
23) M. Iwase, E. Ichise, T. Yamasaki and M. Takeuchi: *Trans. Jpn. Inst. Met.*, **25** (1984), 43.
24) M. Iwase, M. Yasuda and T. Mori: *Electrochim. Acta*, **19** (1979), 261.
25) Y. Kaida, M. Hasegawa, Y. Kikuchi, K. Wakimoto and M. Iwase: *Steel Res. Int.*, **74** (2004), 393.
26) K. Takeuchi, T. Enaka, N. Kon-no, T. Hosotani, T. Orimoto and M. Iwase: *Steel Res.*, **68** (1997), 516.
27) Y. Kaida, M. Hasegawa, Y. Kikuchi, K. Wakimoto and M. Iwase: *Metall. Mater. Trans. B*, **36B** (2005), 43.
28) M. Iwase, E. Ichise and N. Yamada: *Steel Res.*, **56** (1985), 319.
29) S. Seetharaman Ed.: Treatise on Process Metallurgy, Volume 1, Elsevier, Oxford, (2014), 539.
30) H. Yama-Zoye, E. Ichise, H. Fujiwara and M. Iwase: *Trans. Iron Steel Soc. AIME*, **13** (1992), 41.
31) M. Iwase, N. Yamada, H. Akizuki and E. Ichise: *Arch. Eisenhuttenwes.*, **55** (1984), 471.
32) H. Schenck and E. Steinmetz: Wirkungsparameter von Begleitelementen Flüssiger Eisenlösungen und Ihre Gegenseitigen Beziehungen, 2erg. Aufl. Stahleisen Sonderberichte Hef, 7, (1968), 1.